

# Neural network prediction of porosity and permeability of heterogeneous gas sand reservoirs using NMR and conventional logs

G.M. Hamada and M.A. Elshafei

PROFESSIONAL PAPER

**Analysis of heterogeneous gas sand reservoirs is one of the most difficult problems. These reservoirs usually produce from multiple layers with different permeability and complex formation, which is often enhanced by natural fracturing. Therefore, using new well logging techniques like NMR or a combination of NMR and conventional openhole logs, as well as developing new interpretation methodologies are essential for improved reservoir characterization. Nuclear magnetic resonance (NMR) logs differ from conventional neutron, density, sonic and resistivity logs because the NMR measurements provide mainly lithology independent detailed porosity and offer a good evaluation of the hydrocarbon potential. NMR logs can also be used to determine formation permeability and capillary pressure.**

**In heterogeneous reservoirs classical methods face problems in determining accurately the relevant petrophysical parameters. Applications of artificial intelligence have recently made this challenge a possible practice. This paper presents a successful application of Neural Network (NN) to predict porosity and permeability of gas sand reservoirs using NMR T2 (transverse relaxation time) and conventional open hole logs data. The developed NN models use the NMR T2 pin values, and density and resistivity logs to predict porosity, and permeability for two test wells. The NN trained models displayed good correlation with core porosity and permeability values, and with the NMR derived porosity and permeability in the test wells.**

*Key words:* neural network, porosity, permeability, NMR, conventional logs and heterogeneous gas sand reservoirs

## 1. Introduction

Porosity logs measurements require environmental corrections and are influenced by lithology and formation fluids. The porosity derived is the total porosity, which consists of producible fluids, capillary bound fluids and clay-bound water. However, NMR provides lithology independent pore size distribution. Permeability is a measure of fluid rock conductivity. To be permeable, a rock must have interconnected porosity. Greater porosity usually corresponds to greater permeability; however, this is not always the case. Formation permeability is influenced by pore size, shape and continuity, as well as the amount of porosity. Permeability can be determined from resistivity gradients, permeability models based on porosity,  $\phi$ , and irreducible water saturation ( $S_{wi}$ ), formation tester (FT) and nuclear magnetic resonance (NMR). Perhaps, the most important feature of NMR logging is the ability to record a real-time permeability log. The potential benefits of NMR to oil companies are enormous. Log permeability measurements enable production rates prediction and allow optimization of production completion and programs stimulation while decreasing the cost of coring and testing wells especially in heterogeneous tight reservoirs where there is considerable permeability anisotropy.

The field of interest is a gas condensate field producing from a Lower-Mesozoic reservoir. The reservoir is classified as a tight heterogeneous gas shaly sands reservoir. It suffers from lateral and vertical heterogeneity due to diagenesis effect (kaolinite & illite) and variation in grain size distribution. The petrophysical analysis indicates a narrow 8-12% porosity range, and a wide permeability range from 0.01 to 100 mD. Figure 1 shows core porosity-permeability crossplot over whole reservoir section including all facies in different wells. The core data shows cloud of points with undefined trend, which could be roughly subdivided into six or seven regions.<sup>15,1</sup>

In heterogeneous reservoirs, facies may change on few meters and down to few centimetres scales. The average fluid density in this case becomes unsatisfactory due to fluids distribution heterogeneity in the reservoir; thereupon, it is required to explore new porosity determination techniques that are independent of facies change. Due to reservoir heterogeneity; many cores were acquired in different wells covering different reservoir units to create the proper porosity-density and permeability models for each. The uncertainty associated with identification of the proper porosity and permeability model for each unit is high, which could result in high permeability estimation far beyond the actual well performance. Therefore, integration of non standard tools like

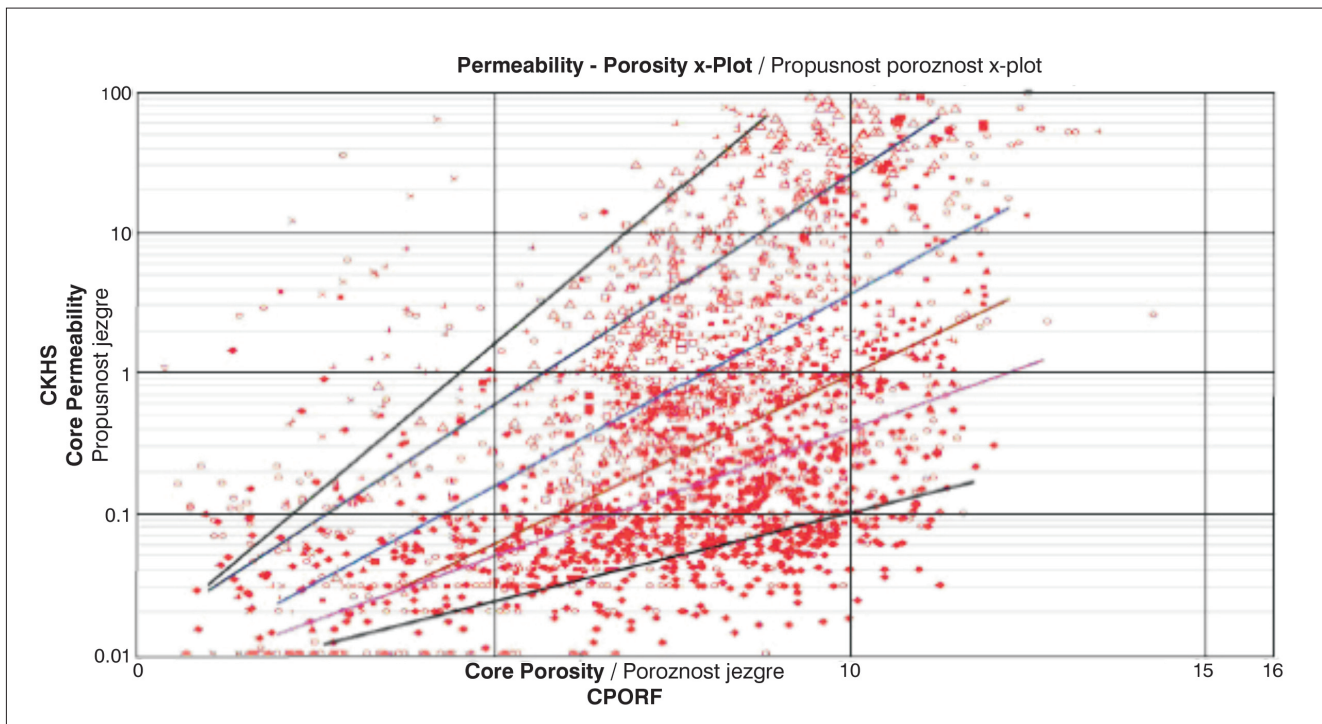


**Fig. 1. Porosity-permeability plot in heterogeneous gas sand**  
Sl. 1. Plot šupljikavost – propusnost u heterogenom plinonosnom pješčenjaku

NMR with conventional tools and special core analysis (SCAL) in the petrophysical evaluation is essential to reduce the uncertainty beyond the limitations of each tool in individual bases, especially in gas reservoirs.<sup>7,18,4</sup>

This work concentrates on determination of porosity ( $\phi_{DMR}$ ) from combination of density porosity and NMR porosity and permeability from NMR logs using Bulk Gas Magnetic Resonance Permeability ( $k_{BGMR}$ ), a technique proposed by Hamada et al<sup>10</sup>, and then using the neural network (NN) technique to predict formation porosity and permeability using NMR and conventional logging data. The NN technique has been developed and applied in several field cases and the predicted porosity and permeability values were validated from the proposed NN algorithm. Predicted porosity and permeability have shown a good correlation with core porosity and permeability in the studied gas sand reservoir.

## 2. Density-magnetic resonance porosity ( $\phi_{DMR}$ )

Freedman et al<sup>6</sup> proposed a combination of density porosity and NMR porosity ( $\phi_{DMR}$ ) to determine gas corrected formation porosity and flushed zone water saturation ( $S_{xo}$ ). Density/NMR crossplot is superior to density/neutron crossplot for detecting and evaluating gas shaly sands. This superiority is due to the effect of thermal neutron absorbers in shaly sands on neutron porosities which cause neutron porosity readings to be too high. As results, neutron/density logs can miss gas zones in shaly sands.<sup>1,6</sup> On the other hand NMR porosities are not affected by shale or rock mineralogy, and

therefore density/ NMR (DMR) technique is the more reliable to indicate and evaluate gas shaly sands.

$$\phi_{NMR} = \phi S_{gxo} HI_g P_g + \phi HI_L (1 - S_{gxo}) \quad (1)$$

### 2.1. Density porosity response in gas flushed zone is defined as

$$\rho_b = \rho_m (1 - \phi) + \rho_L \phi (1 - S_{gxo}) + \rho_g \phi S_{gxo} \quad (2)$$

Solution of equations (1) and (2) for True Formation Porosity ( $\phi$ )

$$\begin{aligned} \phi &= A \cdot \phi_D + B \cdot \phi_{NMR} \\ \phi_{DMR} &= A \cdot \phi_D + B \cdot \phi_{NMR} \end{aligned} \quad (3)$$

where  $\phi_{NMR}$  is NMR porosity,  $HI$  is hydrogen index,  $P$  is NMR polarization,  $\phi_D$  is density porosity,  $S_{gxo}$  is flushed zone gas saturation,  $\rho_b$  is bulk density and  $A$ ,  $B$  are factors.

### 2.2 Calibration for $\phi_{DMR}$ porosity

A curve fitting method has been used to calibrate the  $A$  and  $B$  constants values which are applied to the reservoir of interest. In our case we have selected well (A) (Both core and NMR data were available over the same reservoir interval. Assuming core porosities are equal to  $\phi_{DMR}$ , which is the gas corrected porosity.

Equation (3) can be written in the following form:

$$\frac{\phi_{Core}}{\phi_{NMR}} = A \cdot \frac{\phi_D}{\phi_{NMR}} + B \quad (4)$$

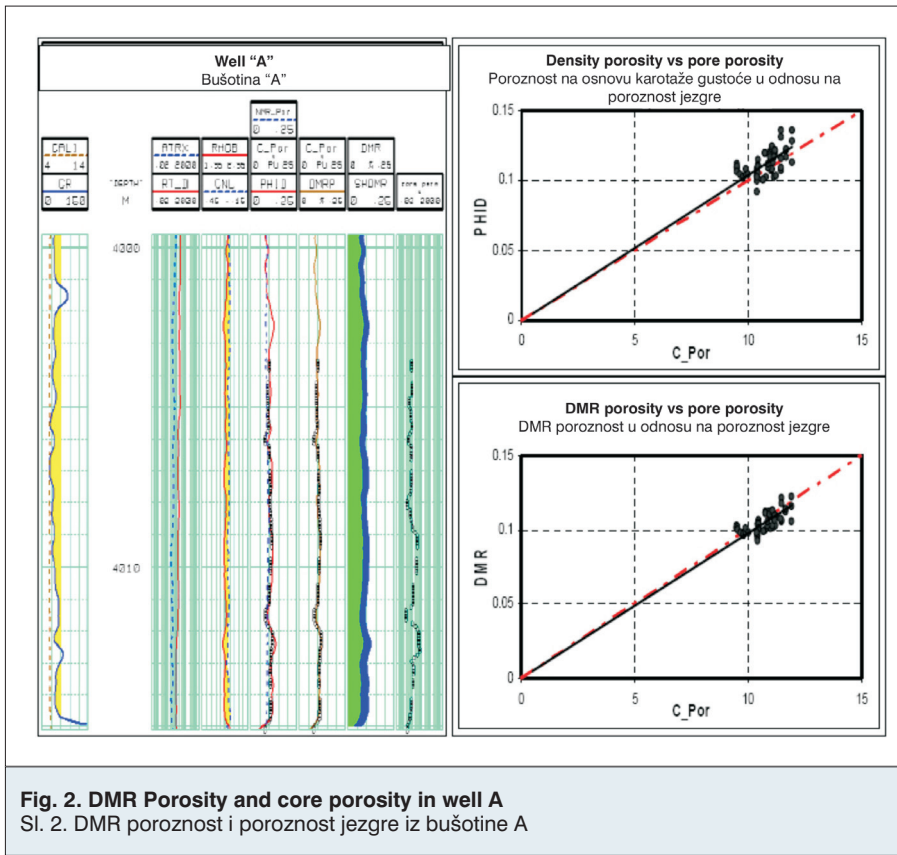


Fig. 2. DMR Porosity and core porosity in well A  
Sl. 2. DMR poroznost i poroznost jezgre iz bušotine A

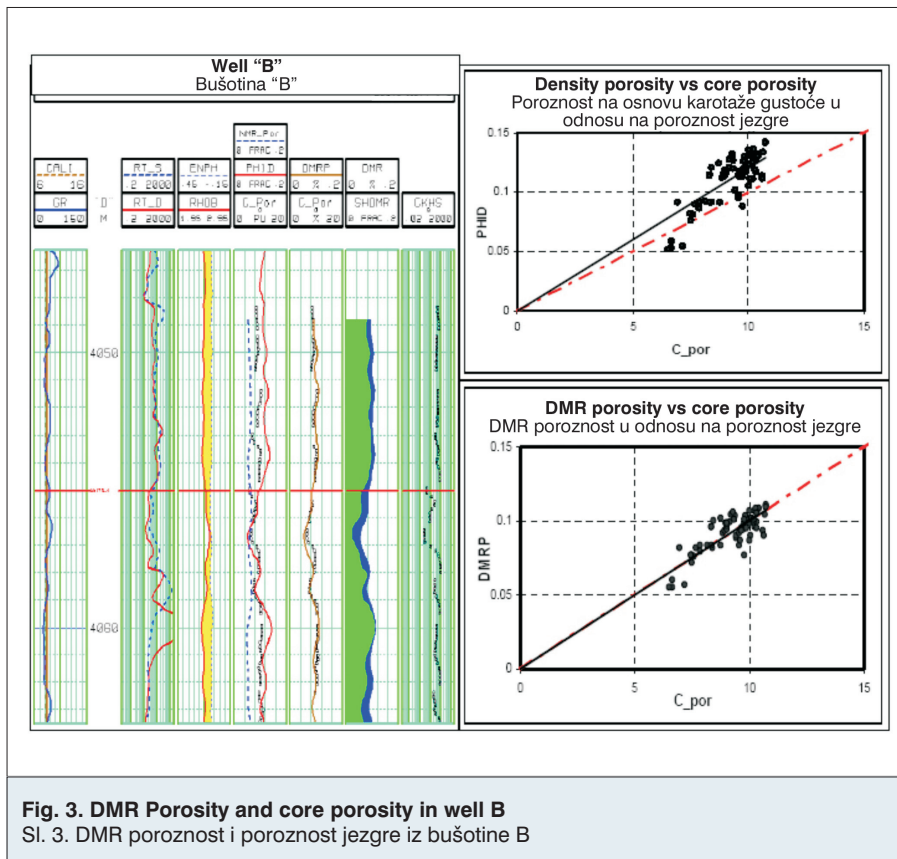


Fig. 3. DMR Porosity and core porosity in well B  
Sl. 3. DMR poroznost i poroznost jezgre iz bušotine B

The fitting trend line has a slope of  $A = 0.65$  and intercepts the  $Y$  axis at  $B=0.35$ , which results in DMR porosity transform as follows

$$\phi_{DMR} = 0.65 \phi_D + 0.35 \phi_{NMR} \quad (5)$$

### 2.3 $\phi_{DMR}$ porosity results

The results of  $\phi_{DMR}$  transform applications in the two test wells A and B showed very good match between  $\phi_{DMR}$  and core porosities as shown in Figures 2 and 3. As a result, it is considered being an independent facies porosity model. These corrected porosities can be used in conjunction with Timur-Coates equation<sup>4</sup> to estimate accurate permeability in gas bearing formations.

Figures 2 and 3 present well logs showing PHID and  $\phi_{DMR}$ . Gamma ray and Caliper curves are shown in the first track (GR and CALI), second track shows depth in meters, the third one is resistivity, the fourth one is neutron-density logs, the fifth track shows comparison between core, density and NMR porosities, the sixth track shows comparison between  $\phi_{DMR}$  and core porosity, the seventh track shows saturations of gas (green shadow) and water (blue shadow) and the last track shows core permeability in mD.

The DMR method has the advantage of avoiding the use of fluid density and gas hydrogen index (HI) at reservoir condition for gas correction. Another advantage is that we can increase logging speeds as we do not need full polarization for gas.<sup>6,13</sup>

### 3. Gas Sand Permeability Estimation from NMR ( $k_{BGMR}$ )

Bulk Gas Magnetic Resonance Permeability ( $k_{BGMR}$ ) is a new technique for permeability estimation in gas reservoirs. It has the same value in oil-based mud (OBM) and water-based mud (WBM) conditions, as it depends on gas re-entry to the flushed zone after mud cake takes place and invasion stops. It is a dynamic concept of gas movement behind mud cake as a result of formation permeability, gas mobility and capillary forces. Be-

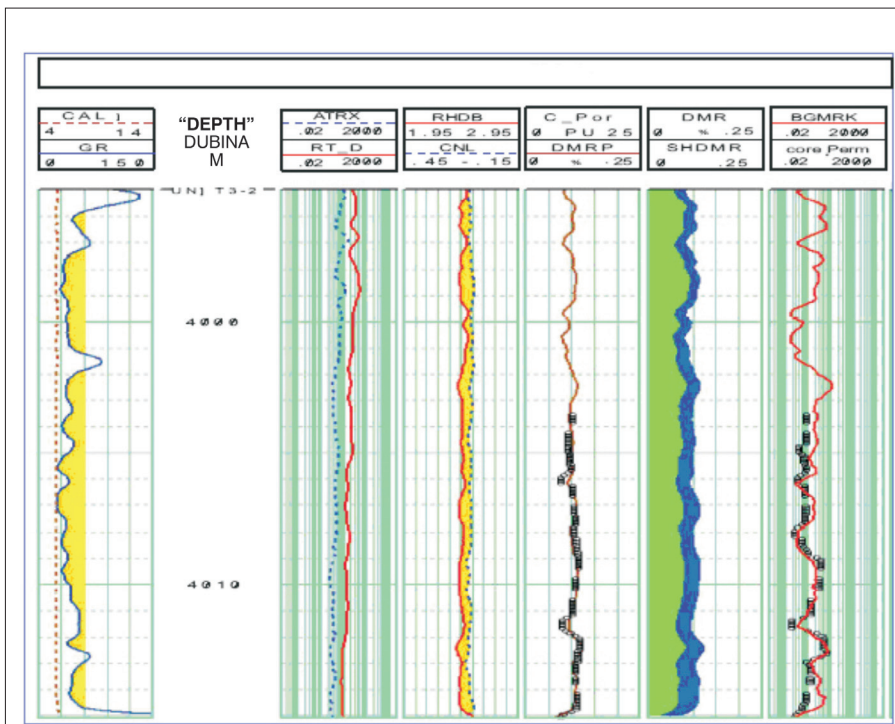


**Fig. 4. Well A, KBGMR permeability, track 6.**  
 Sl. 4. Bušotina A, KBGMR propusnost, krivulja 6

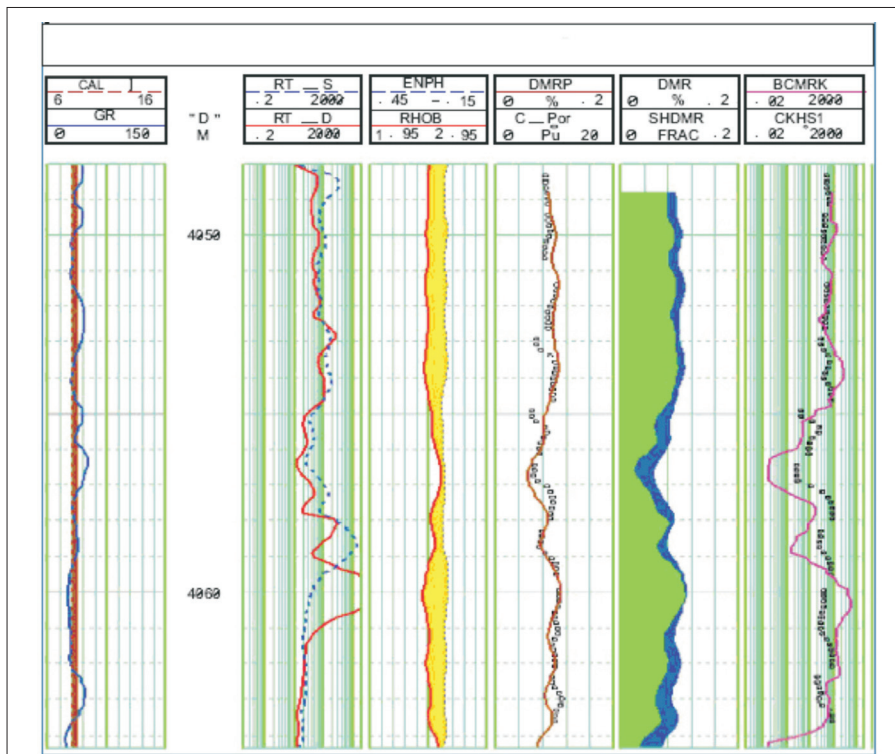


**Fig. 5. Well B, KBGMR permeability, track 6.**  
 Sl. 5. Bušotina B, KBGMR propusnost, krivulja 6

cause gravity forces are constant, capillarity depends mainly on permeability and mobility depends on permeability and fluid viscosity which is constant for gas; the gas re-entry volume is a direct function of permeability.

**3.1 BGM permeability results**

Permeability is derived from empirical relationship between NMR porosity and mean values of T2 relaxation times. Two permeability models are widely used in the industry Kenyon model [ $k=c \cdot \phi_{NMR}^a \times (T2)^b$ ] and Timer-Coates model [ $k = (\phi_{NMR} / c)^a \times (BVM/BVI)^b$ ].<sup>13</sup> Kenyon model permeability is affected by gas and OBM filtrate (non-wetting phase). Timer-Coates permeability model works well in gas reservoirs, but it is affected by uncertainty of BVI cut off values and wettability alteration by OBM filtrate. After defining T2 cut off values, it is time to calibrate the fitting parameters (a, b and c) for studied shaly gas sand reservoir. Permeability determination by Timer-Coates model in the case of tight heterogeneous shaly gas sand was not satisfactory due to the effect of rock facies, tightness and the significant variation of T2 values for the same facies. Estimates of Kenyon and Timer-Coates permeability are both affected by hydrocarbon; therefore, the development of a different permeability model is essential. NMR derived permeability is based on bulk gas volume (BG) in flushed zone. It is the difference between DMR (density magnetic resonance) porosity and NMR porosity.

$$BG \text{ volume} = \phi_{DMR} - \phi_{NMR} \quad (6)$$

The relationship can be normalized by dividing the gas volume by the total porosity of DMRP to be equal to flushed zone gas saturation,  $S_{gxo}$

$$S_{gxo} = (\phi_{DMR} - \phi_{NMR}) / \phi_{DMR} \quad (7)$$

The correlation between  $S_{gxo}$  and permeability in mD has the following form.

$$k_{BGM} = 0.18 \cdot 10^{(6.4qS_{gxo})} \quad (8)$$

Equation (8) has been applied to two wells A and B, where Figures 4

and 5 show the results in the two wells respectively. Wells A, B show a good match between BGMRK permeability with core permeability using the same  $k_{BGMRK}$  transform.

#### 4. NN interpretation of NMR log data

For obvious economic reasons, there has been a paradigm shift in hydrocarbon exploration and development strategies for better utilization of seismic data for reservoir characterization. Discovering the complicated and nonlinear relationship between seismic attributes and reservoir properties has been a major challenge for working geoscientists. Artificial Neural Network techniques have been proposed and proved to be effective in capturing these complex relations, and have proven to be effective modelling tool. Let  $x_1, x_2, \dots, x_5$ , be the input signals,  $w_{k1}, w_{k2}, \dots, w_{kp}$ , are synaptic weights of neuron  $k$ ,  $w_{k0}$  is a bias term,  $v_k$  is the linear combiner output,  $f(\cdot)$  is an activation function, and  $y_k$  is the output signal of the neuron, the mathematical model of the  $k$ -th neuron is described as

$$v_k = \sum_{j=1}^p w_{kj} x_j + w_{k0} \quad (9)$$

$$y_k = f(v_k)$$

The activation function,  $f(\cdot)$ , defines the output of a neuron in terms of the activity level at its input. There are several classes of artificial neural networks structures. The most common structure of ANN is known as multi-layer perceptron Feed Forward Neural Networks (FFNN). FFNNs are composed of layers of interconnected neurons. Usually, an input layer, a number of hidden layers, and an output layer are used as shown in Figure 6. The input layer is essentially a direct link to the inputs of the first hidden layer. The output of each neuron may be connected to the inputs of all the neurons in the next layer. Signals are unidirectional i.e., they flow only from input to output.<sup>11</sup>

The potential of FFNN as a basis for the modeling, classification, and statistical estimation stems from the following characteristics:

- For a sufficient number of hidden units, feed forward neural networks (FFNN) can approximate any continu-

ous static input-output mapping to any desired degree of approximation<sup>11,12</sup>

- Due to the modular and feed forward structure, the training of the network is simple and can be made to adapt to varying conditions.

The back propagation (BP) algorithm is usually used for (FFNN) training.<sup>10</sup> Although BP is simple, the choice of a good learning rate requires some trial and error. Several improved variants of the BP algorithms were proposed in the literature, e.g., the RPROP algorithm, Riedmiller and Braun,<sup>17</sup> Conjugate Gradient, Powell,<sup>16</sup> and Levenberge-Marquardt (LM), Hagan and Menhaj.<sup>9</sup> Although all these algorithms suffer from sensitivity to the initial value of the weights and biases, the LM was shown to be the fastest algorithm for function approximation problems. The LM training algorithm is chosen for training the developed neural networks in this study.

#### 5. Porosity prediction using neural network (NN)

Porosity is a key petrophysical parameter in formation evaluation. Consequently, new well logging techniques are developed to determine accurately formation porosity. Neural networks present an alternative approach to estimate porosity. Soto et al<sup>19</sup> developed a back propagation neural network with four layers to predict permeability and porosity from log data with satisfactory results. Lim and Kim<sup>1</sup> used artificial neural network to classified/identify lithofacies and predicted permeability and porosity from well and he proposed the use of combined fuzzy logic artificial neural network to predict porosity and permeability. Fuzzy curve analysis was used to select the best inputs for the artificial neural network from the available conventional well log data. Elshafei and Hamada<sup>5</sup> estimated formation porosity and water saturation of shaly sand reservoirs with relatively satisfactory result using two separate neural network from well logging measurements.

##### 5.1 NN Porosity prediction using conventional log

The conventional log consists of 5 measurements: Gamma Ray (GR), bulk density (RHOB), Neutron porosity (CNL), Deep and shallow resistivity (RT\_D, and RT\_S). The NMR data consists of 10 T2 pin values. Data from two test wells A and B were combined and split to 60% training and 40% testing. A neural network consisting of 5 inputs, a single hidden layer of 16 neurons, and an output layer was built. The hidden layer consists of a tan-sigmoid function, and the output neuron is a log-sigmoid function. The mean square root error during training, Figure 7 and testing, Figure 8 came to 0.0075 and 0.0102 respectively. The correlation between the predicted values and target values during training came to 0.852, and during

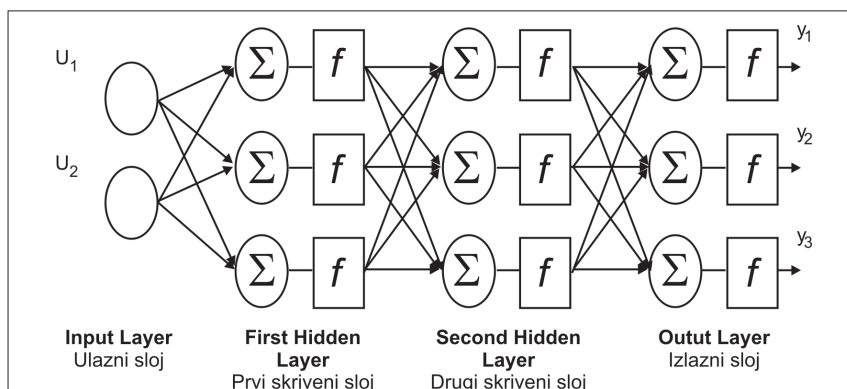
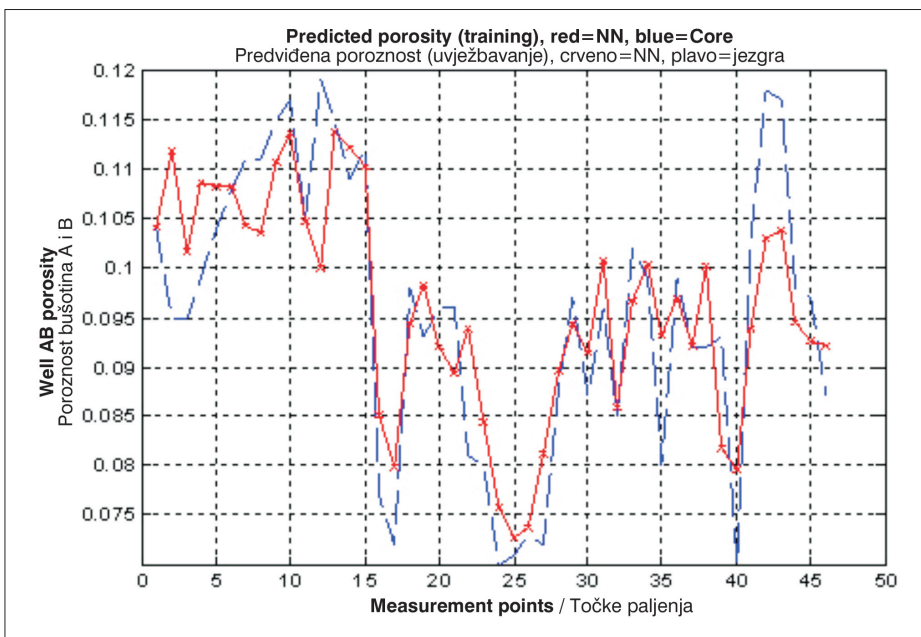
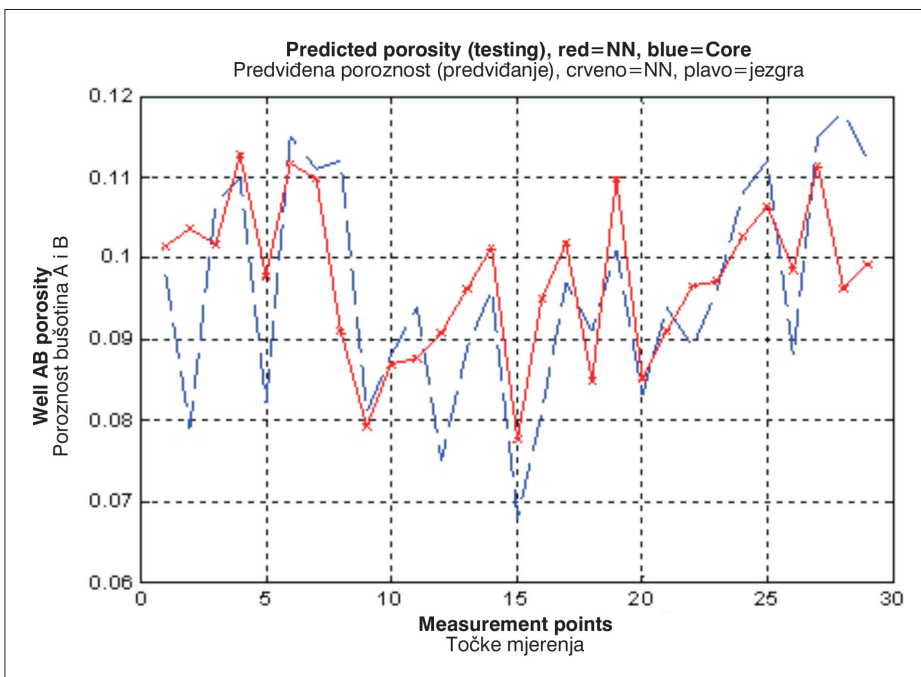


Fig. 6. Multi-layer feed forward neural network (FFNN).  
Sl. 6. Višeslojna Feed-forward neuralna mreža (FFNN)



**Fig. 7. NN prediction of porosity using conventional log, training performance.**  
Sl. 7. NN predviđanje poroznosti korištenjem konvencionalne karotaže, uvježbavanje



**Fig. 8. NN prediction of porosity using conventional log, testing performance.**  
Sl. 8. NN predviđanje poroznosti korištenjem konvencionalne karotaže, predviđanje

testing 0.66. These relatively low correlation coefficients may be attributed to the high noise level in the input data.

### 5.2. NN Prediction of porosity using NMR and conventional log

The data used consists of 5 conventional logs, 10 T2 pins, and the mean value of the pins, the mean squared

value of the pins, and the maximum value of the pins, a total of 18 parameters. Due to the richness of the data, a simple neural network provides an improved performance over the structure used with the conventional log. The neural network here consists of a single hidden layer of 8 neurons. The hidden neurons use tan-sigmoid function, and the output neuron uses a log-sigmoid function.

The root mean square root of errors during training and testing came to 0.0038 and 0.0105 respectively (0.5).

The correlation between the predicted values and target values during training, Figure 9 came to 0.9653 and during testing 0.69. (ff nmr por. net3), Figure 10. The relatively poor performance is mainly due to the small number of core measurements (24 from well A, and 51 from well B, a total of only 75 points).

## 6. Permeability estimation using neural network (NN)

The determination of permeability characteristics is labour intensive and complicated. Empirical models to predict relative permeability from rock and fluid properties have also experienced relatively limited success. Hence alternative methodologies for accurate determination of relative permeability characteristics have since been considered.<sup>19,15,2,3</sup> Artificial neural network (ANN) approach is proposed to predict an accurate permeability. Balan et al<sup>3</sup> did comparative prediction of the permeability estimation from log data using empirical model, multiple variable regression, and artificial neural network. The result shows that multiple regression and neural

network techniques perform better than empirical with neural network as the best tool. Garrouch and Smaoni<sup>8</sup> estimated tight gas sand permeability from porosity, mean pore size, and mineralogical data using a back-propagation neural network model with 8-input neuron and 2-5 hidden layers.

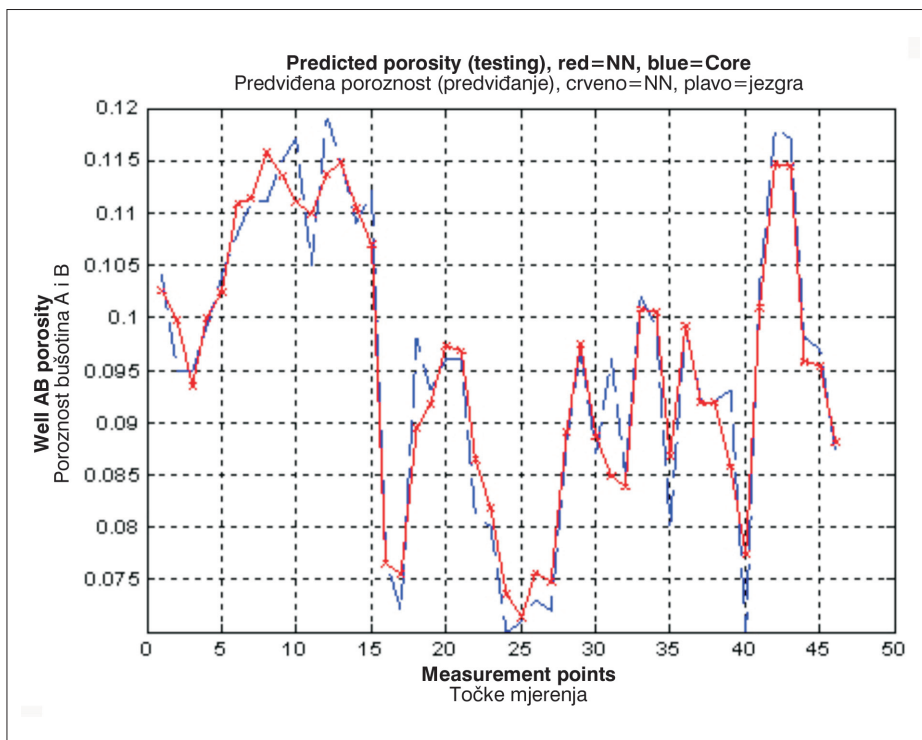


**Fig. 9. NN prediction of porosity using conventional and NMR log, training performance.**  
 SI. 9. NN predviđanje poroznosti korištenjem konvencionalne i NMR karotaže, uvježbavanje

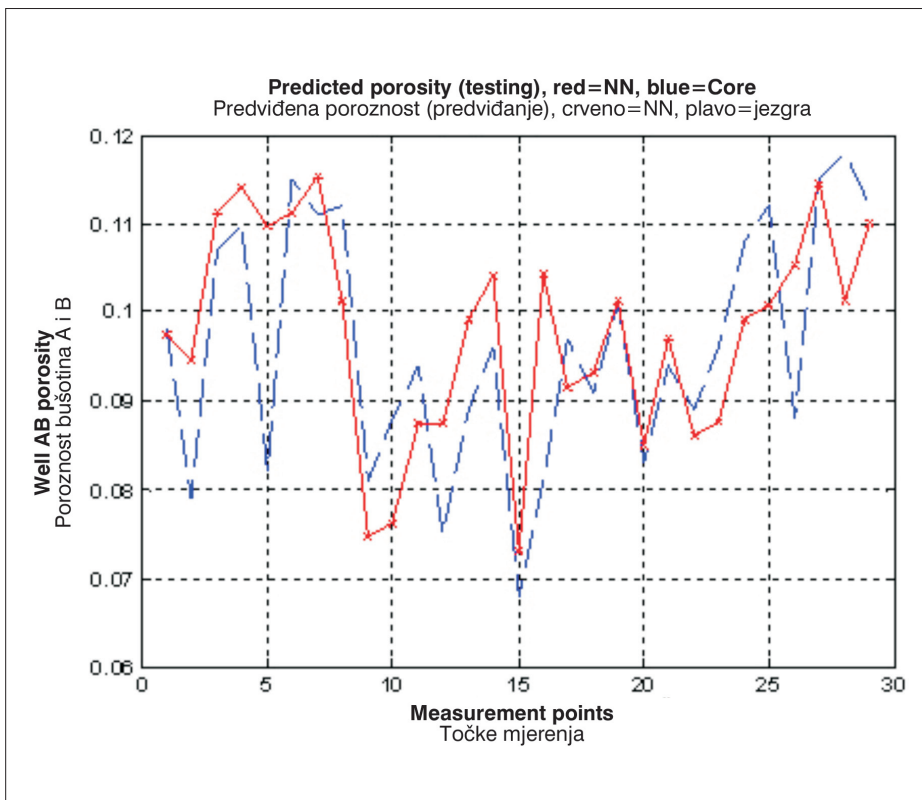


**Fig. 10. NN prediction of porosity using conventional & NMR log, testing performance.**  
 SI. 10. NN predviđanje poroznosti korištenjem konvencionalne i NMR karotaže, predviđanje

### 6.1 Gas sand permeability estimation from NN

Prediction of permeability by Artificial neural network (ANN) approach needs good input logging data, such as NMR data (T2), in addition to conventional logging data (GR, density, Neutron, resistivity). The two wells A, B were analysed to build a NN-based permeability prediction model.

### 6.2 NN permeability prediction using conventional log

Conventional log data from wells A and B were combined and divided into two data sets, a training set of 60% of data, and a test set of 40% of data. It is preferred to start the prediction of permeability using conventional log alone, thereby using Figure 11 as a base line for later assessment of the NMR effectiveness.

The developed NN has five inputs and one hidden layer of 16 neurons. The hidden layer uses tan-sigmoid activation functions, and the output layer uses log-sigmoid activation function. All inputs were normalized between [-1, +1] based on the data available in wells A and B. The permeability was normalized on a log scale as

$$p_n = (\log_{10}(p_{true}) + 2) / 0.5$$

The performance of the developed NN on the training data is shown in Figure 11, and its performance on the test data is shown in Figure 12. The NN achieves a root mean squared error of 6.8 (4.5% of the full-scale) during training, and 9.14 (6.09%) during testing, with correlation coefficient of  $r = 0.9375$ .

### 6.3. NN Permeability prediction using NMR and conventional log

The data used consists of 5 conventional logs, 10 T2 pins, plus the mean value of the pins, the mean squared value of the pins, and the maximum value of the pins, making a total of 18 parameters. The conventional log data and the NMR data from

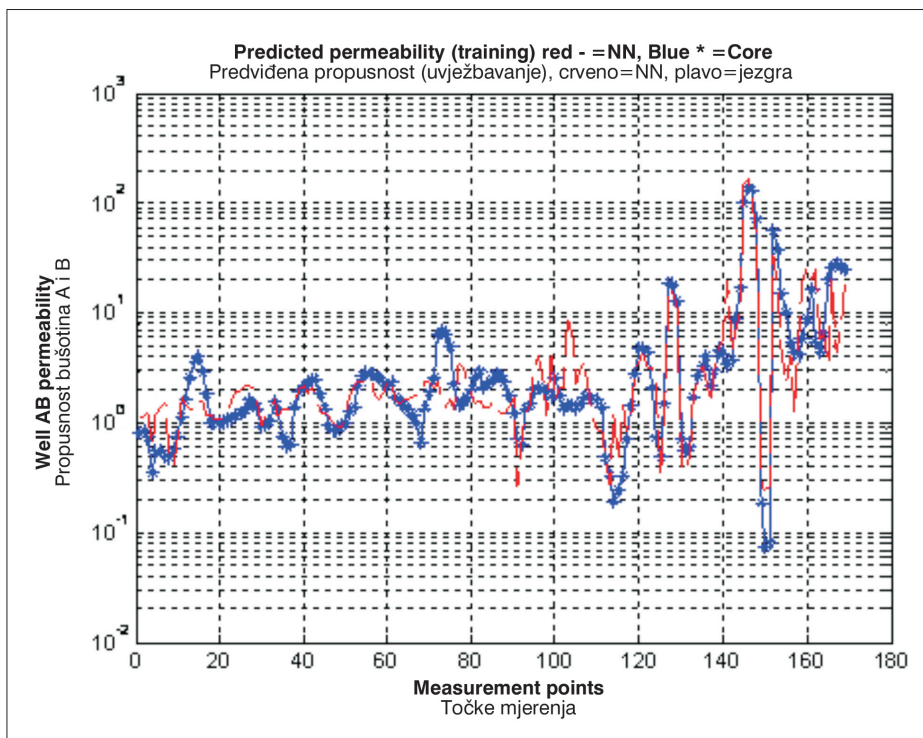


**Fig. 11. NN prediction of permeability using conventional log, training performance.**  
 SI. 11. NN predviđanje propusnosti korištenjem konvencionalne karotaže, uvježbavanje

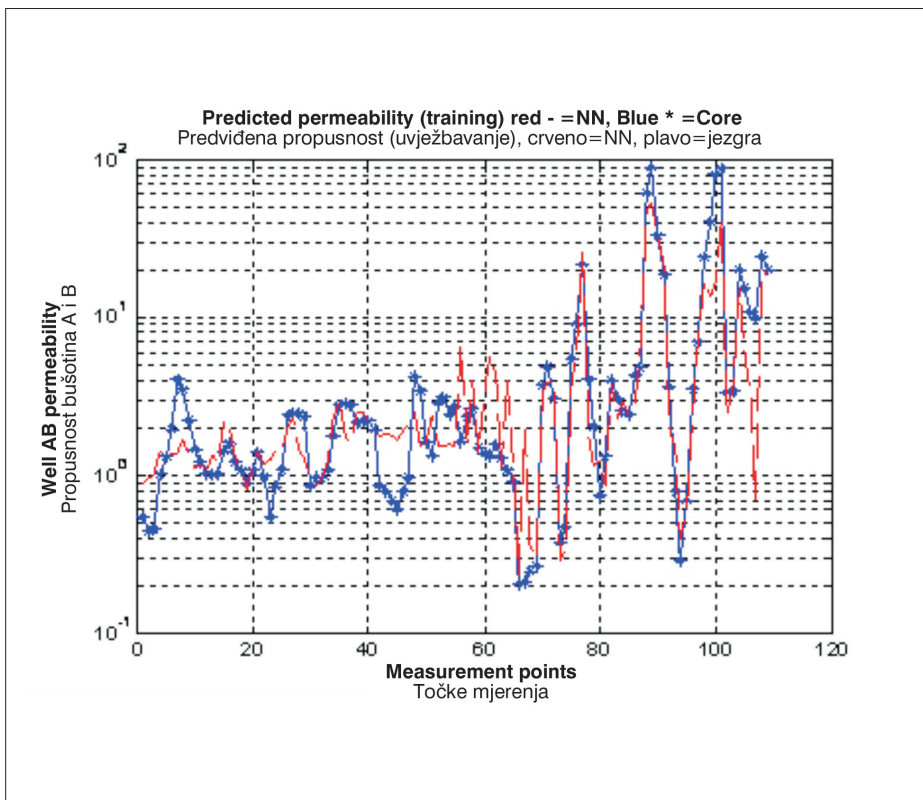


**Fig. 12. NN prediction of permeability using conventional log, testing performance.**  
 SI. 12. NN predviđanje propusnosti korištenjem konvencionalne karotaže, predviđanje

wells A and B were combined and divided into two data sets, a training set of 60% of data, and a testing set of 40% of data.

Due to the richness of the data, a simpler neural network provided an improved performance over the structure used with the conventional log. The neural network here consists of a single hidden layer of 8 neurons. The hidden neurons use tan-sigmoid function, and the output neuron uses a log-sigmoid function. Figure 13 shows the performance of the 18-input NN on the training data, and Figure 14 shows its performance on the test data.

The developed NN achieves a root mean squared error of 4.18 (about 2.8%) and of 4.515 (about 3.01%) on the training data and test data respectively. These results indicate that the NN manages to properly interpolate the test data and achieves almost uniform performance on the entire log data. The correlation coefficient came to  $r = 0.978$  during training, and  $r = 0.961$  during testing.

## 7. Conclusion

1. NMR derived permeability and, porosity have shown good matching with core tests results.
2. NN-predicted porosity using NMR and conventional log has an excellent matching with DMR NMR porosity in training and also in testing sections that indicated an acceptable validation level of NN approach.
3. NN-predicted permeability from NMR decay times T2 and conventional logs achieve very close values to the core permeability.
4. It is recommended to use the developed NN model to predict permeability from NMR data in other wells. It is also recommended to try different NN structures for possibly achieving improved results than those obtained by FFNN.



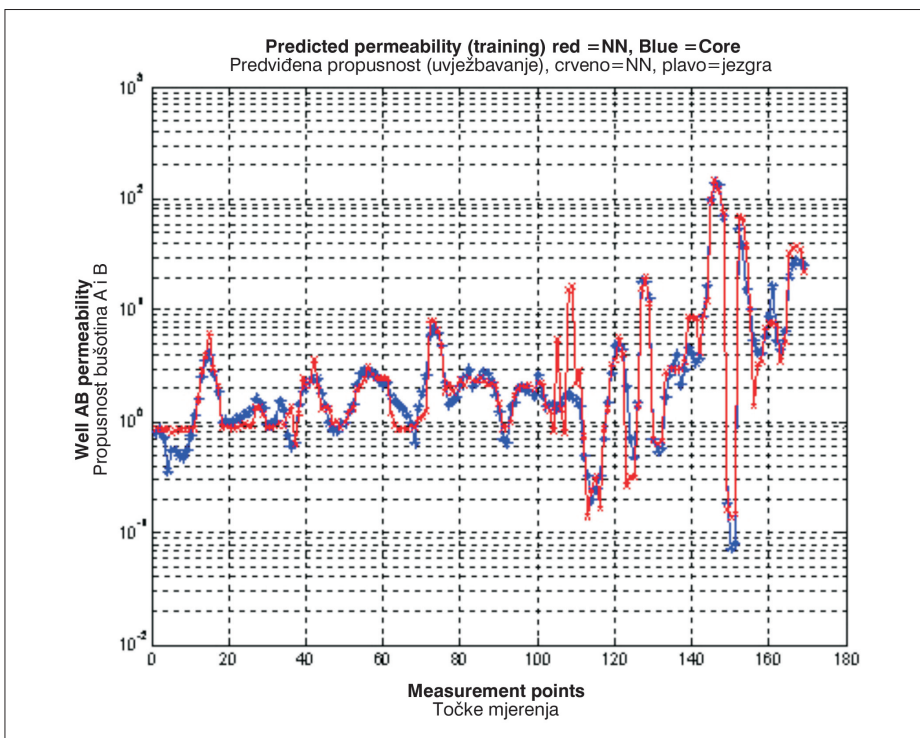


**Fig. 13. NN prediction of permeability using conv. and NMR log, training performance.**  
 SI. 13. NN predviđanje propusnosti korištenjem konvencionalne i NMR karotaže, uvježbavanje

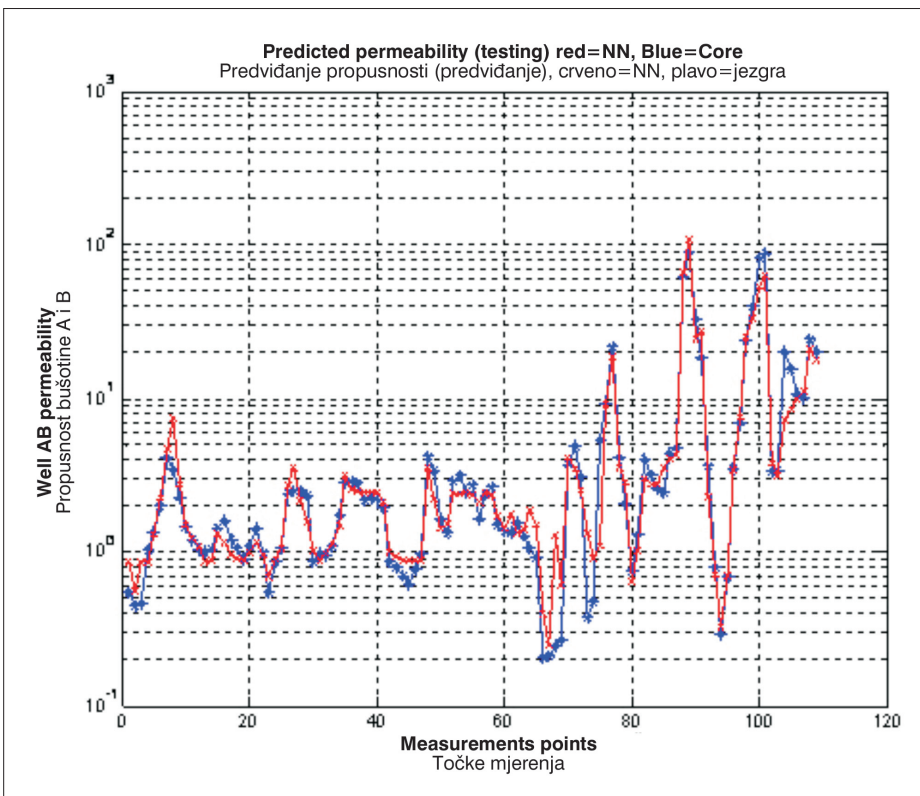


**Fig. 14. NN prediction of permeability using conv. and NMR log, testing performance.**  
 SI.14. NN predviđanje propusnosti korištenjem konvencionalne i NMR karotaže, predviđanje

## Nomenclature

$\phi$	Porosity
$S_{wi}$	Irreducible water saturation
$S_{gxo}$	Flushed zone gas saturation
$FT$	Formation tester
$OBM$	Oil base mud
$WBM$	Water base mud
$PHID$	Density porosity reading
$RT-D$	True resistivity
$RT-S$	Flushed zone resistivity
$NMR$	Nuclear magnetic resonance
$NN$	Neural Network
$BP$	Back propagation training algorithm
$k_{BGMR}$	Bulk gas magnetic resonance permeability
$BG$	Bulk gas volume
$DMR$	Density magnetic resonance
$FFNN$	Feed forward neural network
$LM$	Levenberge-Marquardt training algorithm

## References

1. Abushanab M.A., et al., 2005, DMR technique improves tight gas sand porosity, *Oil & Gas Jr. Dec.*, pp.12-16.
2. Al-Bazzaz, W.H et al, 2007, Permeability modeling using Neural Network approach for complex Mauded-Burgan carbonate reservoir, Paper SPE 105337, Middle East Oil & Show and conference, Manama, Bahrain, 11-14 March.
3. Balan, B., et al, 1995, State of art in permeability determination from well log data: part I-comparative study-model development, paper SPE 30978, SPE Regional Meeting, Canton, USA, 11-14 May.
4. Coates G.R., et al., 1997, Applying total and effective NMR porosity to formation evaluation, Paper SPE 38736, SPE Annual Technical Conference, San Antonio, 11-14 October.
5. Elshafei, M., and Hamada, G.M., 2007, Neural network identification of hydrocarbon potential of shaly sand reservoirs, Paper SPE 110959, SPEKSA Annual Conference, Dhahran, Saudi Arabia, 7-8 May.
6. Freedman R., et al., 1998, Combining NMR and density Logs for Petrophysical Analysis in Gas-Bearing Formations, paper II, SPAWLA 39th Annual Meeting, Colorado, 26-29 May.
7. Galarza T., et al., 2007, Pore-scale characterization and productivity analysis by integration of NMR and openhole logs-A verification study, Paper SPE 108068, Latin American and Caribbean Petroleum Engineering Conference, Buenos Aires, Argentina, 15-18 April.
8. Garrouch, A. and Smaoui, N.H., 1998, An artificial neural network model for estimating tight gas sand permeability, Paper SPE 39703, Asia Pacific Conference on Integrated Modeling for asset Management, Kuala Lumpur, Malaysia, 23-24 March.
9. Hagan, M.T. and Menhaj, M., 1994, Training Feed forward Networks with the Marquardt Algorithm," *IEEE Transaction on Neural Networks*, vol. 5, pp. 989-993.
10. Hamada, G.M., et al., 2008, New NMR approach evaluates tight sand reservoirs, *Oil & Gas J* June 2, pp. 46-53.
11. Haykin, S. *Neural Networks; A 1994, Comprehensive Foundation*, Macmillan Publishing Company, Englewood Cliffs, NJ.
12. Hornik, K., et al., 1989, Multilayer feed-forward network are Universal approximates" *Neural Networks*, v2, p 359-366.
13. Kenyon B., et al., 1995, " Nuclear magnetic resonance imaging-technology for 21st century", Autumn, pp.19-32.
14. Lim, J.S. and Kim, J., 2004, Reservoir porosity and permeability estimation from well log using fuzzy logic and neural network, paper SPE 88476, Asia Pacific Oil and Gas Conference, October 18-20, Perth, Australia
15. Oraby, M.El., et al., 1999, Experiences in permeability calculations in the Obayed field (Egypt) using Magnetic Resonance Imaging, paper SPE 53277, Middle East Oil Show and Conference, Manama, Bahrain, 20-23 February.
16. Powell, M.J.D. 1977, Restart Procedures for the Conjugate Gradient Method," *Mathematical Programming Jr.*, vol. 12, pp. 241-254.
17. Riedmiller, M. and Braun, H., 1993, A Direct Adaptive Method for Faster Back propagation: The RPROP algorithm," presented at Proceeding of the IEEE International Conference on Neural Networks. USA.
18. Riviere Ch. and Roussel J.C., 1992, " Principle and potential of nuclear magnetic resonance applied to the study of fluids in porous media", *Revue IFP*, vol. 47, pp. 503-523.
19. Soto, B., Ferneynes, E.L. and Bejaramo, H., 1997, Neural network to predict the Permeability and porosity of zone C of the Cantagalo field, Colombia, Paper SPE 38134, SPE Petroleum Computer Conference, Dallas, USA, 8-11 June.



Authors:

**G.M. Hamada**, The British University in Egypt (BUE), Egypt

**M.A. Elshafei**, King Fahd University of Petroleum & Minerals (KFUPM), Saudi Arabia